

CONTACT ANALYSIS FOR NONCIRCULAR GEARS

Bogdan CRISTESCU, Laurenția ANDREI, Ana CRISTESCU

Mechanical Engineering Department, Dunarea de Jos University of Galati
cribo_2005@yahoo.com

ABSTRACT

Few studies on the performance of noncircular gears meshing have been produced. Due to their complex geometry and to the lack of standard design procedures, the evaluation of noncircular gear contact and strength is up to researchers and is based both on traditional gear theory and modern computerized methods. The paper presents an investigation of noncircular gears meshing conditions, focused on the static tooth contact and FEM analysis, related to variations in gear tooth geometry. The tooth contact analysis is developed in the AutoCAD environment and describes the paths of contact area and distribution for two gear pairs, generated by the rolling of the rack cutter along the noncircular centrode and along the circular centrode that locally approximates the noncircular centrode, respectively. The FEM analysis is developed by Inventor facilities and enables the evaluation and comparison of the gear tooth stresses and displacements for noncircular gears with various tooth profiles. The results are important to complete the existing noncircular gear data base in an attempt to improve the gear design procedure.

KEYWORDS: noncircular gears, gear generation, gear contact, gear FE analysis

1. INTRODUCTION

Noncircular gears, with complex geometry and kinematics, not designed according to standard procedures, keep challenging the gear industry researchers. As regards noncircular gear generation, there are two main steps to be followed: the modelling of noncircular centrodes and the generation of gear teeth. The first step is usually based on the gear transmission ratio variation [1], [2], [3], the driving centrode geometry [4], [5] or on the law of motion for the driven element [6], [7]. Modelling noncircular centrodes and transferring them into the gear theory, the generation of the gear teeth is further developed by specific analytical approaches that consider the particularities of the gear line of action [8], [9] or the traditional theory of enveloping surfaces [10], [11], and by computerized simulation of the gear cutting process [12], [13]. Usually, the noncircular gear teeth flanks geometry is not an involute, could not be related anymore to a base circle, and varies from one tooth to another and even for the same tooth.

The complex and variable geometry of the noncircular gears leads to particular meshing, with specific problems. The line of action continuously changes its position, the instantaneous contact point

of the mating centrodes being translated along the gears centre line, and its inclination that is related, by a constant or variable pressure angle, to the common tangent of the conjugate noncircular centrodes. Therefore, the noncircular gears meshing behaviour is difficult to predict; few references present different procedures developed for the gear contact performance analysis [14], [15], [16], that put together both the basis of the standard gear geometry and the performance of the computerized methods for the investigation of the gear behaviour.

Considering a general geometry of the gears, with convex-concave zones, the paper is concerned with the study of the noncircular gear static contact performance, manipulating virtual environments. The authors propose two different geometries for the noncircular gear teeth, generated by specific kinematics that are induced by a rolling a rack cutter (i) along the noncircular pitch curve and (ii) along equivalent pitch circles that locally approximate the noncircular arcs. The virtual solid gears are generated based on the interference of the PHP programming language and the AutoCAD application. AutoCAD is also used to simulate the gears meshing and to produce and investigate the tooth static path of contact area and distribution, in relation to the tooth

profile geometry. Imported in Autodesk Inventor, the virtual gear train bending behaviour is investigated, focused on the teeth placed in particular zones of the noncircular pitch curve, i.e. convex zones, with high curvature radius, and in concave zones, critical when the pitch curve exhibits high curvature.

2. GEAR CORRECT AND APPROXIMATE GENERATION

The generation of the noncircular gear teeth is numerically developed by considering the meshing of a standard rack-cutter with the noncircular gear blank; due to the complex geometry of the noncircular centrode, with convex-concave zones, the avoidance of the gear undercutting is assured by considering a “single tooth” rack cutter. In order to analyze or improve the behaviour of the noncircular gears, two different tooth profiles are generated, as resulting from the gear generation hypotheses. To initiate the “cutting” process, each tooth flank is positioned by point E_i , as the intersection point between the current tooth flank profile and the gear noncircular pitch curve (Figs. 1, 2), defined by the polar coordinate φ_i , a multiple of the gear angular pitch. Afterwards, the “cutting” process of each tooth flank is locally developed in its vicinity, as follows:

I. The first hypothesis refers to the correct kinematics of the gear tooth generation. During the rolling motion, the rack cutter pitch line, as a tangent line to the noncircular centrode, continuously changes its inclination, defined by the variable μ_{ij} angle with respect to the current positioning vector $r(\varphi_{ij})$ (Fig. 1).

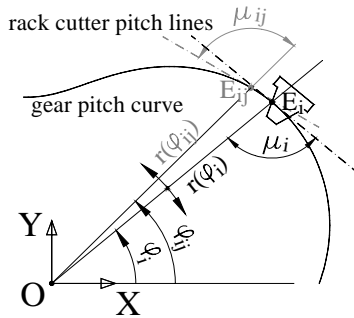


Fig. 1. Correct geometry and kinematics of the noncircular gear tooth flank generation

Considering the rotational motion of the gear blank and the translational motion of the rack cutter tooth during the generating rolling motion, the

$$\begin{aligned} x_{ij} &= r(\varphi_{ij}) \cdot \cos \varphi_{ij} \pm s_{ij} \cdot \cos \alpha \cdot \\ &\cdot \cos(\mu_{ij} + \alpha + \varphi_{ij}), \\ y_{ij} &= r(\varphi_{ij}) \cdot \sin \varphi_{ij} \pm s_{ij} \cdot \cos \alpha \cdot \\ &\cdot \sin(\mu_{ij} + \alpha + \varphi_{ij}) \end{aligned} \quad (1)$$

operating tooth flank is analytically described by the equations (1) where φ_{ij} is the gear rotational angle

about its center O. The (+) sign is used for teeth that are placed in the convex zones of the pitch curves, while the (-) sign is specific for concave zones. The rack displacement during the rolling motion, s_{ij} , is calculated by:

$$s_{ij} = \pm \int_{\varphi_i}^{\varphi_{ij}} \sqrt{r^2(\varphi) + r'^2(\varphi)} d\varphi \quad (2)$$

where the (+) sign is for the tooth addendum generation and (-) sign is for the dedendum generation, respectively. The rack cutter pitch line is inclined by μ_{ij} :

$$\mu_{ij} = \arctg \frac{r(\varphi_{ij})}{\frac{dr}{d\varphi}(\varphi_{ij})} \quad (3)$$

The pressure angle α is constant, chosen at the standard value of 20° .

To complete the tooth generation process, the rotational angle of the pinion extends within $[0, \varphi_{iv}]$ limits, for the addendum flank, and within $[0, \varphi_{if}]$ for the dedendum, where φ_{iv} , φ_{if} are numerically calculated from the equations:

$$\begin{aligned} \int_{\varphi_i}^{\varphi_{iv}} \sqrt{r^2(\varphi) + r'^2(\varphi)} d\varphi &= \frac{1.25 \cdot m}{\sin \alpha \cdot \cos \alpha} \\ \int_{\varphi_{if}}^{\varphi_i} \sqrt{r^2(\varphi) + r'^2(\varphi)} d\varphi &= \frac{m}{\sin \alpha \cdot \cos \alpha} \end{aligned} \quad (4)$$

Similar equations describe the opposite (passive) tooth flank profile:

$$\begin{aligned} x'_{ij} &= r(\varphi'_{ij}) \cdot \cos \varphi'_{ij} \pm s_{ij} \cdot \cos \alpha \cdot \\ &\cdot \cos(\mu_{ij} - \alpha + \varphi'_{ij}), \\ y'_{ij} &= r(\varphi'_{ij}) \cdot \sin \varphi'_{ij} \pm s_{ij} \cdot \cos \alpha \cdot \\ &\cdot \sin(\mu_{ij} - \alpha + \varphi'_{ij}) \end{aligned} \quad (5)$$

where φ'_{ij} is the incremental gear rotational angle in the vicinity of the passive tooth flank, positioned at angle $\varphi'_i = \varphi_i + 0.5\pi m$ (m is the gear modulus) along the gear pitch curve.

A general noncircular centrode geometry, with convex-concave zones, leads to unknown curves for the tooth flank profile, actually the involute of a local noncircular curve, which will further be mentioned as the CG (correctly generated) profile.

II. The second hypothesis generates the tooth operating flank, positioned by the E_i point, as it belongs to a spur gear whose pitch circle locally approximates the noncircular pitch curve (Fig. 2).

During the rolling motion, the rack cutter tooth is translated along its pitch line, with constant inclination, μ_i , with respect to the current positioning vector $r(\varphi_i)$:

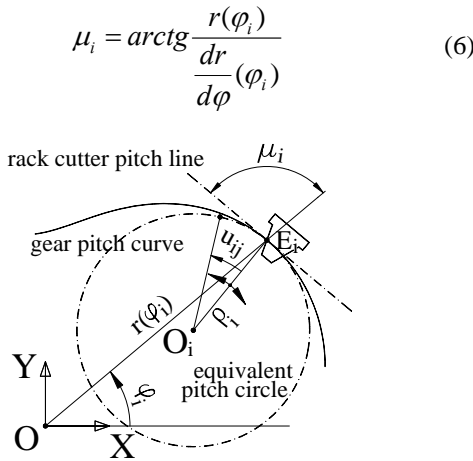


Fig. 2. Approximate geometry and kinematics of the noncircular gear tooth flank generation

The inclination of the rack cutter pitch line obviously varies from one tooth to another and from one tooth flank to another. The rotational motion is performed by the equivalent spur gear, with ρ_i pitch radius, about its center O_i . The tooth operating flanks are analytically described by Eq. 7, where u_{ij} is the equivalent spur gear rotational angle about its center. The (\pm) sign is used for teeth generated in convex and concave zones of the pitch curves, respectively.

$$\begin{aligned} x_{ij} &= r(\varphi_i) \cdot \cos \varphi_i \pm \rho_i \cdot \sin(\varphi_i + \mu_i) \\ &\mp \rho_i \cdot \sin(\varphi_i + \mu_i - u_{ij}) \mp \rho_i \cdot u_{ij} \cdot \\ &\cos \alpha \cdot \cos(\varphi_i + \mu_i - u_{ij} - \alpha), \\ y_{ij} &= r(\varphi_i) \cdot \sin \varphi_i \mp \rho_i \cdot \cos(\varphi_i + \mu_i) \\ &\pm \rho_i \cdot \cos(\varphi_i + \mu_i - u_{ij}) \mp \rho_i \cdot u_{ij} \cdot \\ &\cos \alpha \cdot \sin(\varphi_i + \mu_i - u_{ij} - \alpha) \end{aligned} \quad (7)$$

Similar equations describe the opposite tooth flank profile:

$$\begin{aligned} x'_{ij} &= r(\varphi'_i) \cdot \cos \varphi'_i \pm \rho_i \cdot \sin(\varphi'_i + \mu_i) \\ &\mp \rho_i \cdot \sin(\varphi'_i + \mu_i - u_{ij}) \mp \rho_i \cdot u_{ij} \cdot \\ &\cos \alpha \cdot \cos(\varphi'_i + \mu_i - u_{ij} + \alpha), \\ y'_{ij} &= r(\varphi'_i) \cdot \sin \varphi'_i \mp \rho_i \cdot \cos(\varphi'_i + \mu_i) \\ &\pm \rho_i \cdot \cos(\varphi'_i + \mu_i - u_{ij}) \mp \rho_i \cdot u_{ij} \cdot \\ &\cos \alpha \cdot \sin(\varphi'_i + \mu_i - u_{ij} + \alpha) \end{aligned} \quad (8)$$

where $\varphi'_i = \varphi_i + 0.5\pi m$.

The second hypothesis of the noncircular gear generation leads to involute profiles for the gear tooth flanks, the involute of the local equivalent spur gears.

These profiles will further be mentioned as the AG (approximately generated) profiles.

Figure 3a shows the noncircular centrode and the tooth flank profiles of a pinion that belongs to a gear pair defined by the gear transmission ratio from Eq. 9 and the number of teeth $z_l = 36$. The calculus is developed by the original PhP codes and the graphical

representation is performed with AutoCAD facilities. The tooth flanks are generated by both of the above mentioned hypotheses.

$$m_{21}(\varphi) = 1 + \frac{1}{4} \cdot \cos \varphi + \frac{1}{3} \cdot \sin 3\varphi \quad (9)$$

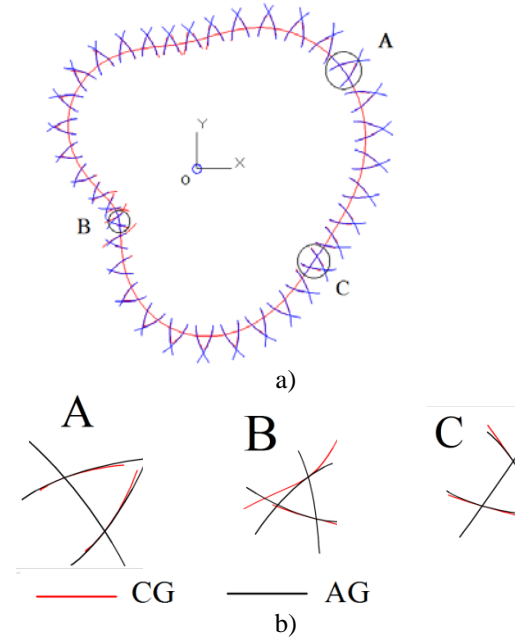


Fig. 3. Noncircular gear centrode and CG, AG profiles of the tooth flanks (a), geometrically compared in details (b)

Figure 3b enables a geometrical comparison between the profiles of these tooth flanks; three significant teeth are chosen to numerically analyze their profiles, i.e. the teeth placed in centrode zones with convex geometry and reduced curvature (A), with concave geometry and high curvature (B) and nearly linear geometry (C). The results show that the tooth profile deviation rises towards the tooth top and root, in relation with the centrode curvature. In centrode zones, with high curvature, the AG profile has higher curvature than the CG profile and leads to a smaller tooth thickness. As the centrode curvature radius is increased, the AG profile records reduced curvature and get outside the CG profile.

To numerically evaluate the differences between the CG tooth and the AG profiles, the geometrical points defining the curves are listed (Table 1) and a data base is created, leading to a “tooth profile deviation” estimated by:

$$\Delta_{ij} = \sqrt{(x_{ij} - x'_{ij})^2 + (y_{ij} - y'_{ij})^2} \quad (10)$$

It is found that the tooth placed in the convex zone of the noncircular pitch curve, with high curvature radius (A tooth), records smaller profile deviations at the tooth root (a medium of $7.95 \mu m$) compared with those recorded at the tooth top (a

medium of 10.39 μm); the tooth placed in the concave zone of the noncircular pitch curve, with small curvature radius (B tooth), records a medium tooth profile deviation of 10.68 μm for the root, compared with 12.58 μm, a medium value calculated at the tooth top; tooth specific to the nearly linear zone of the noncircular pitch curve records a profile deviation of 10.41 μm at the tooth root and of 9.36 μm at the tooth top.

Table 1 presents a sequence of data recorded for the A, B, C tooth flank profiles, in points defined at the tooth profile top (point 19) and root (point 1) and at the intersection with the gear pitch curve (point 10).

Table 1. Tooth profiles data base and deviations for noncircular gear CG and AG profiles

	Points		
	1	10	19
Tooth A – convex pitch curve, small curvature			
x_{ij} [mm]	412.36	420.88	426.32
y_{ij} [mm]	219.42	219.66	218.94
x'_{ij} [mm]	425.70	420.88	406.75
y'_{ij} [mm]	218.42	219.66	218.78
Δ_{ij} [μm]	13.38	0.00	19.57
Tooth B – concave pitch curve, high curvature			
x_{ij} [mm]	559.14	560.03	558.65
y_{ij} [mm]	310.60	299.14	295.99
x'_{ij} [mm]	557.60	560.03	560.62
y'_{ij} [mm]	292.33	299.14	319.72
Δ_{ij} [μm]	18.34	0.00	23.81
Tooth C – linear pitch curve			
x_{ij} [mm]	213.64	210.81	201.42
y_{ij} [mm]	232.93	232.46	227.19
x'_{ij} [mm]	196.26	210.81	216.47
y'_{ij} [mm]	225.06	232.46	233.36
Δ_{ij} [μm]	19.08	0.00	16.27

3. TOOTH CONTACT ANALYSIS

In order to investigate the noncircular gears meshing, virtual solid models are manipulated. Basically, to generate a noncircular gear train, based on the predefined gear transmission ratio m_{21} , initial complementary data is requested (the gear center distance D and the number of teeth for the pinion and driven gear, z_1 and z_2 , respectively) and editing operations should be applied using CAD applications.

A gear train defined by the gear transmission ratio in Eq. 9 is generated. The conjugate pitch curves are easily modeled and the PhP codes enable to numerically describe the tooth flanks of the pinion

(Eqs. 1, 5, Fig. 3a) and driven gears. For the analytical description of the driven gear tooth flanks, the coordinate transformation method is applied (Fig. 4, Eq. 11). Imported in AutoCAD, the data base enables the gears sections to be illustrated. In order to produce the solid virtual gears, the editing operations assume that the addendum and dedendum curves are offsetting the pitch curves at standard distances of m and $1.25m$, respectively, the root fillet radius being chosen as $0.25m$.

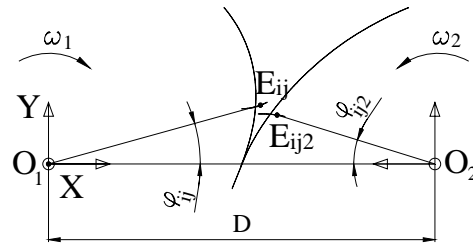


Fig. 4. Generation of the conjugate tooth flank of the driven gear

$$\begin{bmatrix} x_{ij2} \\ y_{ij2} \end{bmatrix} = \begin{bmatrix} D \\ 0 \end{bmatrix} + \begin{bmatrix} \cos \varphi_{ij2} & \sin \varphi_{ij2} \\ -\sin \varphi_{ij2} & \cos \varphi_{ij2} \end{bmatrix} \cdot \left(\begin{bmatrix} x_{ij} \\ y_{ij} \end{bmatrix} - \begin{bmatrix} D \\ 0 \end{bmatrix} \right) \quad (11)$$

where

$$\varphi_{ij2} = \int_0^{\varphi_{ij}} m_{21}(\varphi) d\varphi \quad (12)$$

Figure 5 illustrates a noncircular gear train with $z_1 = z_2 = 36$, the gear center distance is 200 mm and the gears facewidth is 20 mm. For the static tooth contact analysis, the pinion tooth B is chosen as the “critical” gear tooth.

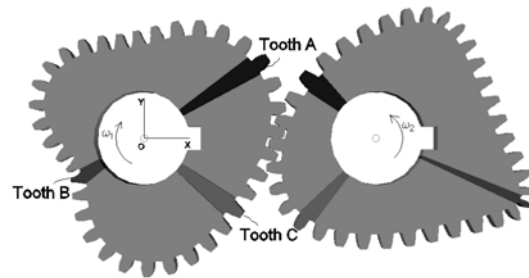


Fig. 5. Noncircular virtual gears, highlighting the tooth pairs subjected to contact analysis

To produce and analyze the tooth contact, the following algorithm is considered:

1. The tooth pair conjugate flanks are got into mesh at the instantaneous contact point, on the gear center line, considered as the reference position;
2. The pinion is initially rotated, by 0.001°, to produce a small interference with the driven gear;

3. The pinion is clockwise incrementally rotated by an angle of 1° , while the driven gear is rotated by the correspondent rotational angle, imported from the PhP codes (Eq. 12). The intersection of solids produces, for each position, the tooth path of contact whose evolution along the gear tooth addendum is recorded (path area and distribution) (Fig. 6);

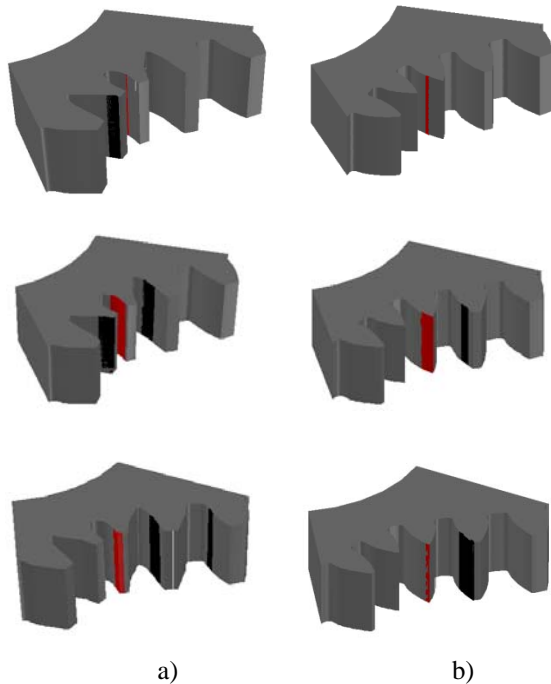


Fig. 6. Producing the tooth static contact path on ANCG gear (a) and ANAG gear (b)

4. The gears are back rotated to the reference position and a new meshing process is initiated by an incremental counterclockwise rotational motion, to produce the tooth contact path specific to dedendum zone. The procedure also enables to pick up the rotational angles where the tooth comes into and gets out of mesh.

The algorithm is applied for both gear trains, correctly (ANCG) and approximately (ANAG) generated, to compare the influence of the tooth profiles on the meshing conditions. Table 2 presents a selection of the B tooth contact path data, i.e the number of teeth in contact, the area of contact path on the B tooth (BCA) as well as the total path of contact (TCA). The data recorded are subject to the AutoCAD precision in generating and manipulating operations.

The pinion B tooth is in mesh within the angular limits $[207^\circ, 221^\circ]$, for both gear trains. The ANCG gear train starts the B tooth meshing with two teeth in contact and rapidly engages in mesh a third tooth, while the ANAG gear train exhibits single and double contacts. The mesh starts with a reduced area and increases the contact path area during the rotational motion of the gears. The ANCG gear train records a higher contact surface than the ANAB gears, the maximum value, usually got in point on the

gear center line, being twice as that specific to involute tooth profiles.

Table 2. Tooth contact parameters in the vicinity of B pinion tooth

Pinion rotational angle	$\varphi_1 = 207^\circ$	$\varphi_1 = 209^\circ$	$\varphi_1 = 221^\circ$
ANCG – correctly generated			
Nr. Teeth	2	3	3
BCA [mm ²]	47.706	176.739	74.635
TCA [mm ²]	108.815	380.354	201.912
ANAG – approximately generated			
Nr. Teeth	1	2	2
BCA [mm ²]	32.835	157.002	52.404
TCA [mm ²]	32.835	209.220	142.751

Other teeth, placed in the convex zones (Fig. 7), have similar behaviour leading to the conclusion that the gears generated by correct geometry and kinematics exhibit higher tooth contact while meshing.

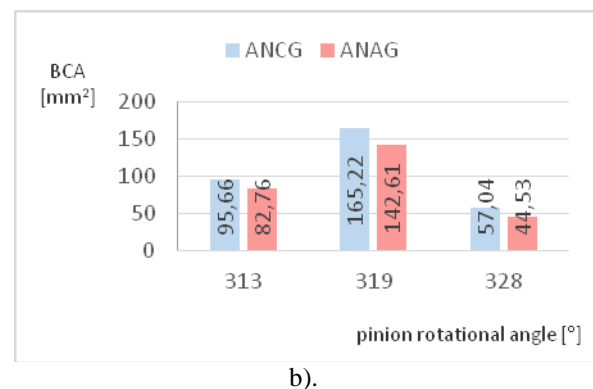
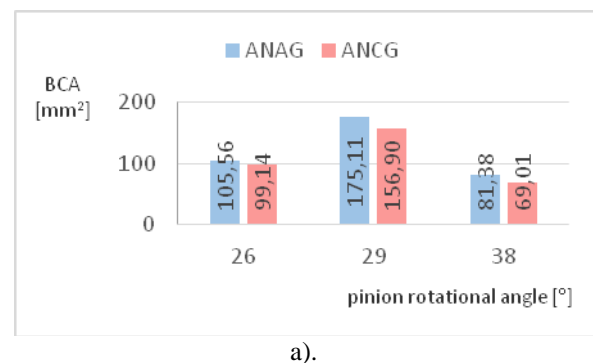


Fig. 7. Tooth static contact path area, measured on pinion A tooth (a) and C tooth (b), for ANCG and ANAG gear trains

4. TOOTH FEM ANALYSIS

The FEM analysis is applied to the previously generated noncircular gear train, focused on the influence of the tooth flank geometry on the gear bending stresses and deflections, in static conditions. The analysis is developed using the procedures of the

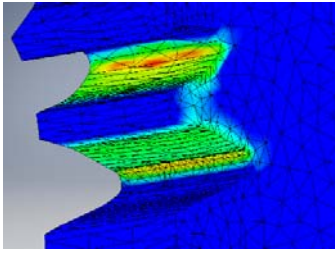
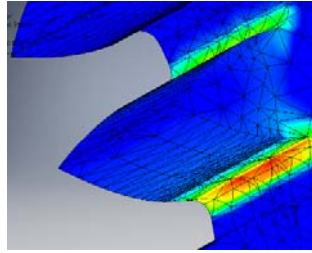
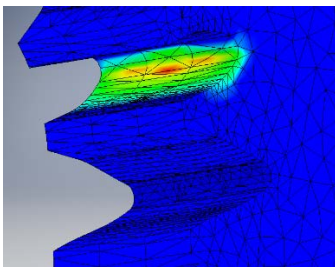
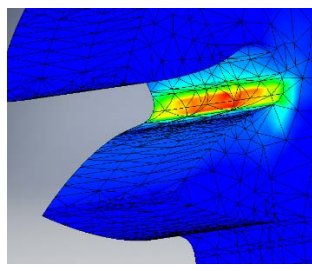
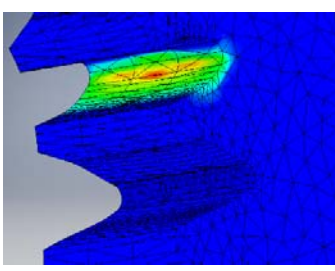
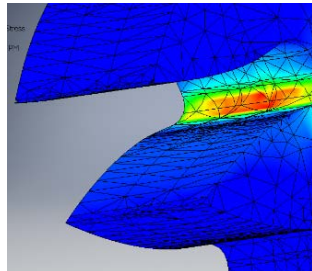
Autodesk Inventor, based on conventional hypotheses applied for standard gears [17].

The following considerations are taken into account: the gear is made by Aluminium 6061-T6, it is rotated about OZ axis, a force of 10 N is applied, uniformly distributed along the gear facewidth, at the

B tooth top, while single into mesh; the force is applied along the current line of action whose inclination is calculated by a PHP code. The structure of the finite elements is chosen as follows:

- the average size of the element is 0.1, related to the overall model size;

Table 3. Tooth stresses and deflections on the gear concave zone (tooth B)

Von Mises stress distribution			
ANCG		ANAG	
			
First principal stress distribution			
ANCG		ANAG	
			
Tooth deflection			
ANCG		ANAG	
			

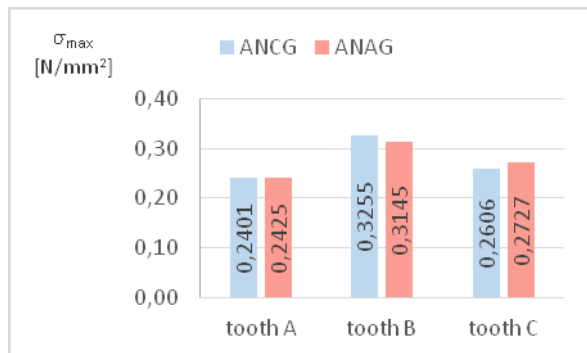
- the minimum size of the element is 0.2, related to the average size;
- the maximum rotational angle of the element is 60°;
- there are 257503 nodes and 167286 elements.

In Table 3, the distribution of the stresses and deflections for the B tooth of the pinion, part of the ANCG and ANAG noncircular gears train, is shown. The results show superior performance recorded for the B tooth, located in the concave section of the pinion generated by approximate method (ANAG). Thus, the maximum value of the Von Mises stress, recorded for the ANAG gear, is 3.51 % higher

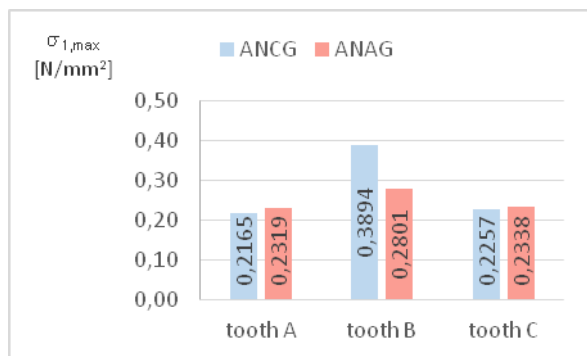
compared to the ANCG gear and the maximum displacement is increased by 14.87 %, respectively (Fig. 8).

The gear virtual models are generated by the predefined gear ratio hypothesis, chosen to induce complex gear geometry, with convex, concave and linear segments of the gear pitch curve. Two methods for the gear tooth generation are considered, using the rolling of a standard rack-cutter tooth along the noncircular centrode and along a pitch circle arc that locally approximates the noncircular centrode, respectively. The slightly different tooth geometries

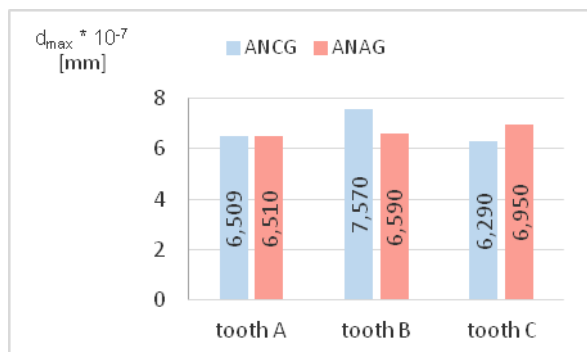
are taken into account for the investigations upon the noncircular gears meshing.



a).



b).



c).

Fig. 8. Comparison of Von Mises maximum stresses in gear teeth (a), first principal stresses (b) and deflections (c), for ANCG and ANAG gear trains

As regards the bending behaviour of the teeth placed in the convex zones (Fig. 8), it is found that, for the Von Mises Stress and the tooth deflection, the maximum values recorded are generally lower for the ANCG gear. Comparing to ANAG gear, the decrease of the Von Mises maximum stress value is of 0.9% for tooth A, specific to convex pitch curve, and of 4.4% for tooth C, from linear pitch curve; the tooth deflection is reduced by 0.02% for tooth A and by 5.17% for tooth C.

5. CONCLUSIONS

The noncircular gears contact analysis is developed simulating the gears meshing under static conditions.

The static analysis of meshing aims at the contact between the teeth and the state of tooth stresses and deflections in required areas, i.e. the convex area, with large radius of curvature, and the concave area, with small radii.

The teeth contact is evaluated based on contact path size and distribution, in AutoCAD environment, simulating the incremental rotational motion of the gears during the contact between two chosen conjugated teeth. The results highlight that the correct generation of the teeth, by rolling the rack cutter along the noncircular centrod, provides larger contact surfaces and multiple tooth engagements, compared with the approximate generation method.

The tooth bending analysis, developed under static conditions, by the Autodesk Inventor finite element procedures, reveals that the correctly generated gear exhibits better meshing conditions for the rectilinear and convex areas, by reducing the maximum values of Von Mises stress and of the tooth displacement, while the approximately generated gear records lower stress and deflection for tooth of gear concave zone.

The results of noncircular gear contact performance enable improvement of the gears design, managing the tooth profile geometry through varying the gear generation geometry and kinematics.

ACKNOWLEDGEMENT

The work has been funded by the Sectoral Operational Programme Human Resources Development 2007-2013 of the Ministry of European Funds through the Financial Agreement POSDRU/159/1.5/S/132397.

REFERENCES

- [1] Quintero Riaza, H.F., Foix, S.C., Nebot, L.J., *The synthesis of an N-lobe noncircular gear using Bézier and B-spline nonparametric curves in the design of its displacement law*, Journal of Mechanical Design, v 129, 2007, September, pag 981-985;
- [2] Mundo, D., *Geometric design of a planetary gear train with non-circular gears*, Mechanism and Machine Theory, v 41, 2006, pag 456-472;
- [3] Cristescu, A., Cristescu, B., Andrei, L., *Designing Multispeed Gear Pitch Curves*, Applied Mechanics and Materials, v 657, 2014, pag 480-484;
- [4] Bair, B.-W., Chen, C.-F., Chen, S.-F., Chou, C.-Y., *Mathematical Model and Characteristic Analysis of Elliptical Gears Manufactured by Circular-Arc Shaper Cutters*, Journal of Mechanical Design, v 129, 2007, February, pag 210-217;
- [5] Andrei, L., Vasie, M., *Using supershape in noncircular gear centrod modeling process*, The Annals of "Dunarea Jos" University of Galati, Fascicle II, Mathematics, Physics, Theoretical Mechanics, n 2, 2010, pag 259-266;
- [6] Laczik, B., *Involute Profile of Non-Circular Gears*, <http://igor.chudov.com/manuals/Non-Circular-Gears.pdf>;

[7] **Mundo, D., Gatti, G., Dooner, D.B.**, *Combined synthesis of five-bar linkages and non-circular gears for precise path generation*, 12th IFToMM World Congress, 2007;

[8] **Litvin, F.L.**, *Noncircular Gears Design and Generation* [Book], 2009, Cambridge University Press;

[9] **Cristescu, B., Andrei, L., Cristescu, A.**, *Analytical generation of involute flanks of noncircular gear tooth*, The Annals of "Dunarea Jos" University of Galati, Mathematics, Physics, Theoretical Mechanics, Fascicle II, Year VI (XXXVII), v 1, 2014, pag 104–110;

[10] **Laczk, B., Zentay, P., Horváth, R.**, *A New Approach for Designing Gear Profiles using Closed Complex Equations The Method of Gear Profile Generation*, Acta Polytechnica Ungarica, v 11, 2014, n 6, pag 159–172;

[11] **Danieli, G.A.**, *Analytical Description of Meshing of Constant Pressure Angle Teeth Profiles on a Variable Radius Gear and its Applications*, Journal of Mechanical Design, v. 122, 2000, March, pag 123-129;

[12] **Bair, B.W.**, *Computer aided design of elliptical gears with circular-arc teeth*, Mechanism and Machine Theory, v 39, 2004, pag 153–168;

[13] **Vasie, M., Andrei, L.**, *Noncircular gear design and generation by rack cutter*, The Annals of "Dunarea Jos" University of Galati, Technologies in Machine Building, Fascicle V, 2011, pag 81–86;

[14] **Khan, S.**, *Simulation and analysis of transmission error in helical non circular gear model*, IJMET, v 6, 2015, n 2, pag 128–136;

[15] **Barkah, D., Shafiq, B., Dooner, D.**, *3D Mesh Generation for Static Stress Determination in Spiral Noncircular Gears Used for Torque Balancing*, Journal of Mechanical Design, v 124, 2002, June, p. 313-319;

[16] **Cristescu, A., Cristescu, B., Andrei, L.**, *Finite element analysis of multispeed noncircular gears*, Applied Mechanics and Materials, v 808, 2015, pag 246-251;

[17] **Conatantin, V., Palade, V.**, *Mecanisme si organe de masini* [Book], 2005, Editura Fundatiei Universitatea 'Dunarea de Jos' Galati.